FULL PAPER

Carbon Nanotube Based Multifunctional Ambipolar Transistors for AC Applications

Zhenxing Wang, Zhiyong Zhang, Hua Zhong, Tian Pei, Shibo Liang, Leijing Yang, Sheng Wang, and Lian-Mao Peng**

Field-effect transistors (FETs) fabricated on large diameter carbon nanotubes (CNTs) present typical ambipolar transfer characteristics owing to the small band-gap of CNTs. Depending on the DC biasing condition, the ambipolar FET can work in three different regions, and then can be used as the core to realize multifunctional AC circuits. The CNT FET based circuits can work as a high-efficiency ambipolar frequency doubler in the ambipolar transfer region, and also can function as in-phase amplifier and inverted amplifier in the linear transfer region. Due to current saturation of the CNT FET, an AC amplifier with a voltage gain of 2 is realized when the device works in the linear transfer region. Achieving an actual amplification and frequency doubling functions indicates that complicated radio frequency circuits or systems can be constructed based on just one kind of device: ambipolar CNT FETs.

1. Introduction

Recently, tremendous progress has been achieved on carbon based nanoelectronics, including carbon nanotubes (CNTs) and graphene.[1–3] Provided with ultrahigh carrier mobility and saturation velocity as well as ultrathin body, both of CNTs and graphene have been appealing for high frequency electronics,[3–10] especially for the applications of ambipolar electronics, which takes advantages of the unique characteristic of carbon based transistor comparing with conventional devices. Utilizing ambipolar transport characteristic, some kinds of AC integrated circuits, including frequency doublers, mixers, phase detectors, and digital modulators, have been realized based on graphene field-effect transistors (FETs).[11–16] Besides graphene, CNTs with small band-gap (SBG) also present ambipolar transfer properties and can be used to build ambipolar frequency doubler with better performance potentially owing to its higher mobility and smaller dimension.[17] However, the operating principle of the ambipolar electronics determines that the FET has to work at the small transconductance region which is centered at the zero transconductance point (ZTP, also known as Dirac point in graphene). Moreover, the FET with small transconductance even near zero presents a considerably low voltage gain far below 1, i.e., a serious signal attenuation.[11,12,16,17] Therefore, voltage amplifiers are necessary to cascade to the ambipolar circuits (such as frequency doubler or mixer) so as to make sure the amplitude of the output signal is large enough for the next level circuit in practical applications. In other words, both of the ambipolar transistors for constructing signal processing circuits and the linear transistors for constructing voltage amplifiers are indispensable blocks in RF ICs for actual applications. To avoid the increase of fabricating process and cost, a preferred choice is to realize the amplifier on the same type of devices for constructing the frequency transforming circuits. Although graphene transistors have demonstrated multifunctionality under triple modes, the actual amplifying function has still not been realized.[16] It is well known that voltage amplifier is difficult to achieve on graphene FETs, in which the current saturation cannot be realized easily and requires a complicated process, such as embedded back-gate and ultrathin high-κ dielectric, to make the gapless single layer graphene behave saturation property at room temperature.[18] Compared with graphene FETs, CNT FETs, including SBG CNT FETs, easily present current saturation in output characteristics.[17] Meanwhile, SBG CNTs with large diameter are promising materials for radio frequency applications owing to their ultrahigh mobility which mainly comes from the fact that the substrate scattering is highly suppressed owing to the cylinder structure, superior to graphene, which suffers strong substrate scattering.[17,19,20] Thus, multifunctional FETs can be fabricated on SBG CNTs to construct radio frequency integrated circuits, in which AC gain amplifiers can be realized on FET via biasing the device to the linear region, and ambipolar frequency transforming circuits can be realized on the same FET via biasing it in the ambipolar region centered at ZTP. Although in previous work, we only focused on the ambipolar CNT FET functionalized as a frequency doubler, the current saturation properties were negleted. Therefore, these devices were not designed or biased to realize amplification.

In this work, we demonstrate a multifunctional SBG CNT FET for radio frequency applications. The device presents typical

Dr. Z. X. Wang, Dr. Z. Y. Zhang, H. Zhong, T. Pei, S. B. Liang, L. J. Yang, Dr. S. Wang, Prof. L.-M. Peng
Key Laboratory for the Physics and Chemistry of Nanodevices and Department of Electronics, Peking University, Beijing 100871, China
E-mail: zyzhang@pku.edu.cn; lmpeng@pku.edu.cn

DOI: 10.1002/adfm.201202185

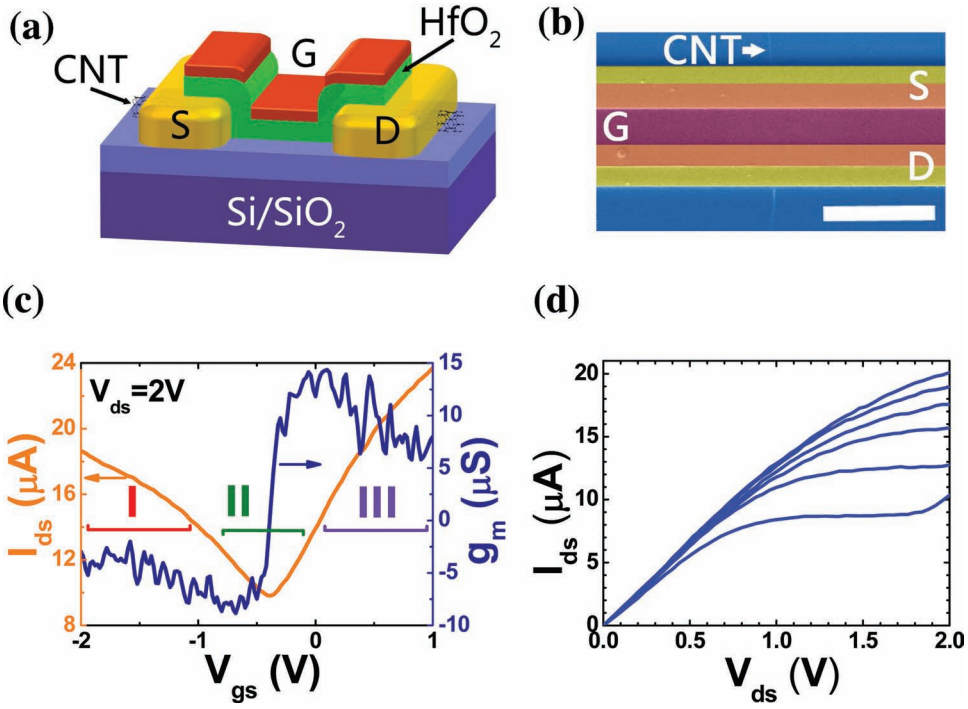

Figure 1. Geometry and DC characteristics of a small band gap CNT FET. a) Schematic diagram showing the geometry of the self-aligned top gated CNT device. b) SEM image showing the top view of a real device, in which colors indicate the different layers. The channel length is about 2 μm, and the scale bar is 5 μm. c) DC transfer characteristic and gate voltage dependent transconductance. Depending on the gate voltage, the transfer curve may be divided into 3 regions, corresponding to different working modes. d) Output characteristics of the device at the n-branch. V_{gs} varies from –0.5 to 1 V with a step of 0.3 V from bottom to top.

ambipolar transfer characteristics owing to the small band gap, and then is used to as a frequency doubler, in-phase amplifier, and inverted amplifier. The transition between different modes may be made easier via changing simply the DC bias voltage level. Particularly, the amplifier can attain an AC voltage gain of greater than 2, which means that an actual voltage amplification (gain>1) is realized in the multifunctional carbon-based nanodevices.

2. Results and Discussion

2.1. Ambipolar Transfer Property of CNT FETs

Figure 1a shows the geometry of a CNT FET which adopts a well developed self-aligned gate structure,[21] and its SEM image is shown in Figure 1b. The channel length is about 2 μm, and the diameter of the CNT is about 5 nm, as measured through atomic force microscopy. Since the band-gap is inversely proportional to the diameter in semiconducting CNTs, diameter of about 5 nm will lead to a band-gap of approximately 140 meV, which is small enough to present obviously ambipolar transfer characteristic especially modulated by high-efficiency top gate at room temperature.[22] Transfer (I_{ds}–V_{gs}) curves of the SBG CNT FET were measured under biasing V_{ds} of 2 V as shown in Figure 1c, which clearly indicates typical ambipolar transfer characteristics, and then the gate voltage dependent transconductance was derived via the differential of the transfer curve. The gate voltage of minimum current point (or ZTP) $V_{gs\text{-}ZTP}$ is about –0.4 V, which is the transition point between n-branch and p-branch. At the region with V_{gs} smaller than $V_{gs\text{-}ZTP}$, the current increases with decreasing V_{gs}, and FET is at the p-branch. While at the region with V_{gs} larger than $V_{gs\text{-}ZTP}$, the current increases with increasing V_{gs}, and FET is at the n-branch. It is obvious that the FET based on individual CNT presents large transconductance both in n-region and p-region, i.e., the maximum transconductance reached as high as about 9 and 14 μS in the p- and n-regions, respectively. It should be noted that the output curve (I_{ds}-V_{ds}) shows current saturation at high bias, as shown in Figure 1d. The current saturation indicates that the device presents large AC output resistance and then can be used to construct a voltage amplifier with high gain.

Depending on the conductance type, the transfer curve of the CNT FET is divided into three regions, i.e., Regions I, II, and III from left to right. Region II is ambipolar, centered at the minimum transconductance point, while the curves in Regions I and III are monotonic, with negative and positive maximum absolute transconductance points, respectively. The CNT FET can be used to realize different functions when biased at different regions, and can be referred as a multifunctional device.

2.2. Working Principle of the Multifunctional Circuit

The working principle of the CNT FET based multifunctional circuit are demonstrated in **Figure 2**, in which the gate

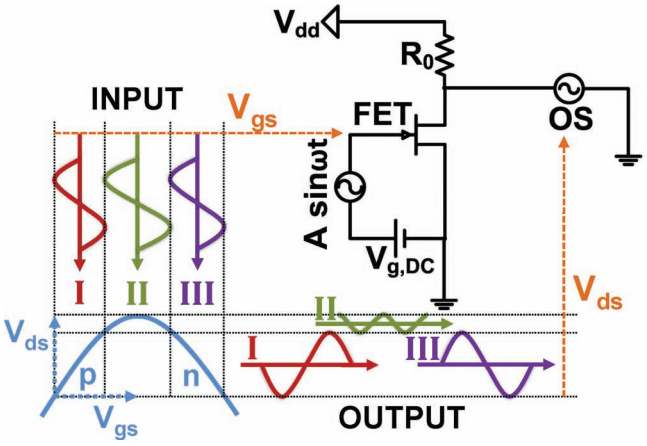

Figure 2. Operation principle of the multifunctional CNT FET based AC circuit. When applying a biased sinusoidal signal at the gate electrode as input, different output signals are obtained depending on the DC biasing condition on the gate electrode. The device performs as an in-phase amplifier in Region I, a frequency doubler in Region II, and an inverted amplifier in Region III.

(G) electrode serves as the input port, and the drain (D) electrode serves as the output port, with the source (S) electrode is grounded. When a sinusoidal signal is applied at the input port, the gate voltage can be written as

$$V_{gs} = V_{g,DC} + A\sin\omega t, \tag{1}$$

where $V_{g,DC}$ is the DC biased at the gate and determines the working region of the FET. The output signal detected by an oscilloscope (OS) is a dropped voltage based on the applied voltage V_{dd} via an external load resistor R_0, and is given by

$$V_{ds} = V_{dd} - I_{ds} R_0, \tag{2}$$

where the drain-source current I_{ds} through the FET is controlled by the gate voltage V_{gs}, such that $I_{ds} = f(V_{gs})$, as shown in Figure 1c. Hence, the relation between output V_{ds} and input V_{gs} is

$$V_{ds} = V_{dd} - f(V_{gs}) R_0 \tag{3}$$

Utilizing the different I_{ds}–V_{gs} relations at different gate regions, we can obtain different functional circuits. If the input signal is biased to the minimum transconductance point, the device alternately works in the p- and n-regions, i.e., region II. When the device works in the p-region, a complete period will appear in the output signal, whereas in the n-region, there is another complete period in the output, and finally frequency doubling is realized.[12] This can also be expressed assuming a parabolic relation for the I_{ds}–V_{ds} curve in Region II, i.e.,

$$I_{ds} = f(V_{gs}) = B + C(V_{gs} - V_{gs,DC})^2 \tag{4}$$

with B and C being two constant coefficients. For a sinusoidal input wave at the input port, the output signal can be deduced by substituting Equation (4) into Equation (3) to obtain

$$V_{ds} = V_{dd} - B R_0 - \frac{1}{2} R_0 C A^2 + \frac{1}{2} R_0 C A^2 \cos 2\omega t. \tag{5}$$

It may be concluded from Equation (5) that a perfect frequency doubling function can be realized if the device works in Region II.

If the input sinusoidal signal is biased to Region I or III, I_{ds}–V_{gs} obeys a linear relation,

$$I_{ds} = f(V_{gs}) = D + g_m (V_{gs} - V_{gs,DC}), \tag{6}$$

where g_m is the transconductance of the transistor, i.e., the slope of linear region, and is negative in Region I and positive in Region III. For a sinusoidal input wave at the input port, the output signal can be deducted by substituting Equation (6) from Equation (3) to yield

$$V_{out} = V_{dd} - D R_0 - g_m R_0 A \sin\omega t \tag{7}$$

It can be seen from Equation (7) that a linear voltage amplifying function can be realized when the transistor operates in Region I or III, and the voltage gain is given by

$$A_v = \frac{\partial V_{out}}{\partial V_{in}} = -g_m R_0. \tag{8}$$

Equation (8) gives the voltage gain of an ideal transistor in which the output resistance of the FET is infinitely great. However, the output resistance, R_{out}, is a finite value in practical FETs, and real voltage gain, A_v, of the circuit is given by[23]

$$A_v = -g_m \frac{R_{out} R_0}{R_{out} + R_0} \tag{9}$$

The input biased in Region I, i.e., $g_m < 0$, the gain is positive and the device works as an in-phase amplifier, although there exists a little phase difference between the input and output due to the delay in the device. On the contrary, if the input is biased in Region III, we have a positive transconductance and the gain is negative, thus the device is turned into an inverted amplifier, via simply altering the bias condition. The conclusions above can also be reached using the projection method via the transfer curve, as shown in Figure 2.[12,17]

2.3. The Frequency Doubling Function

The AC multifunctions are then demonstrated based on the ambipolar transistor, and the AC test setup is according to the circuit diagram in Figure 2. At first, the CNT FET was biased in Region II, and the ambipolar frequency-doubling function was measured. The gate of the CNT FET was biased with a DC voltage $V_{g,DC}$ = –0.4 V, i.e., at the minimum transconductance point. During the frequency doubling measurements, we adopted a series resistor (R_0 = 400 kΩ) as the load and applied V_{dd} = 3 V at the drain electrode. When an input sinusoidal signal with frequency of 1 kHz was applied at the gate electrode, the sinusoidal output signal with a frequency of 2 kHz was measured, as shown in **Figure 3**a. Therefore, frequency doubling was achieved with a gain of almost 120 mV/800 mV = 0.15, which is larger than that of the graphene frequency doubler.[11,12,16] The output power spectrum, as shown in Figure 3b, was obtained through Fourier transforming the time domain output signal in Figure 3a. This power spectrum shows that most of the output RF power (about 90%) is concentrated at the

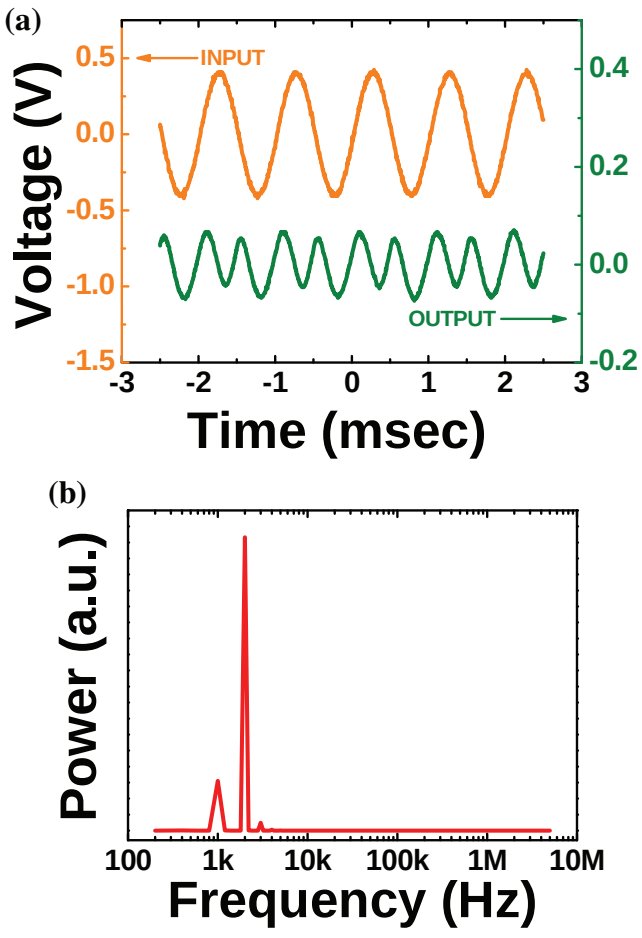

Figure 3. Frequency doubler characteristics of the circuit shown in Figure 1. a) Input and output waveforms for biasing at Region II, where the DC bias (V_{gs}) is –0.4 V. The input signal frequency is 1 kHz, and the circuit works as a frequency doubler. b) Power spectrum obtained via fast Fourier transforming (FFT) of the output time domain signal in (a).

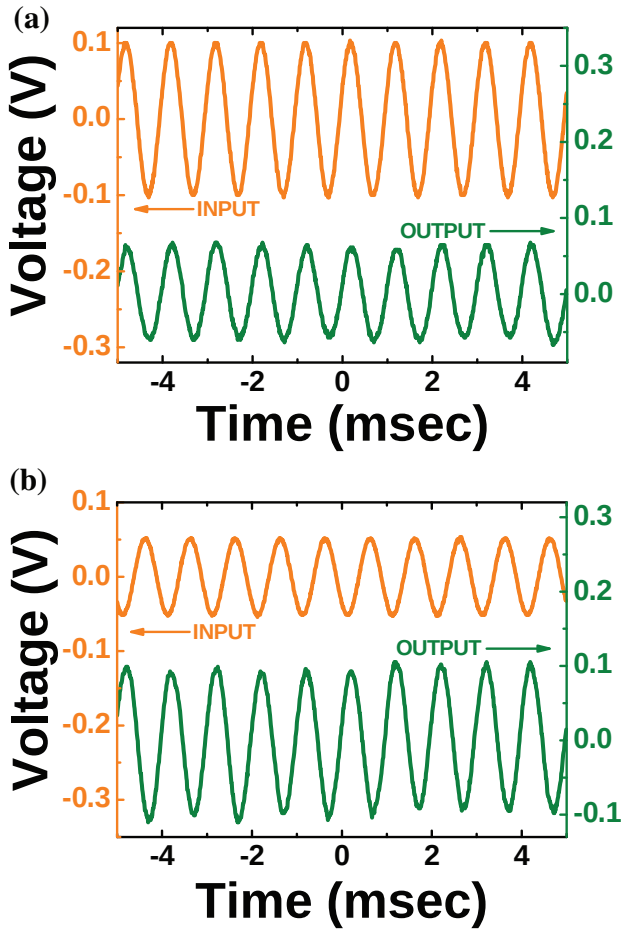

Figure 4. Amplifier characteristics of the circuit shown in Figure 1. a) Input and output waveforms for biasing in Region I, where the DC bias (V_{gs}) is –1.2 V. The input signal frequency is 1 kHz, and the circuit works as an in-phase amplifier. b) Input and output signal for biasing in Region III, where the DC bias (V_{gs}) is 0.1 V. The input signal frequency is 1 kHz, and the circuit works as an inverted amplifier.

doubled fundamental frequency of 2 kHz. This high frequency doubling conversion efficiency comes from the almost perfect ambipolar characteristic of the CNT-FET based on SBG.

2.4. The AC Amplifying Function

AC voltage amplifying is an indispensable function in analog applications,[18,23] and can also be obtained from the CNT FET biased in Region I or III. The circuit functions as an in-phase amplifier as shown in **Figure 4**a, when the CNT FET is biased at $V_{g,DC} = -1.2$ V, i.e., the device works in Region I. If an input sinusoidal signal with frequency of 1 kHz and peak-to-peak voltage ($V_{in,pp}$) of 200 mV was applied on the gate electrode, the output signal is the in-phase sinusoidal wave with the same frequency and peak-to-peak voltages of 130 mV as shown in Figure 4a. The in-phase amplifier is with a voltage gain of about 0.65, which is smaller than unity; therefore, a real amplifying function is still not obtained. When the CNT FET is biased at $V_{g,DC} = 0.1$ V and $V_{dd} = 12$ V, the transistor works in Region III and the circuit in Figure 2 is expected to act as an inverted voltage amplifier. When an input sinusoidal signal with frequency of 1 kHz and amplitude of 100 mV was applied at the gate electrode, an output signal is the antiphase sinusoidal wave with the same frequency and amplitude of 200 mV, as shown in Figure 4b. It is a remarkable fact that a voltage gain of about 200 mV/100 mV = 2 is obtained, which means an actual amplification can be operated based on CNT FET based devices. The actual voltage gain is achieved due to the saturated output of the CNT FET, as shown in Figure 1d. The saturated output characteristics indicate a large AC output resistance, R_{out}, which is essentially a key parameter for an FET to present voltage gain according to Equation (9). Although multifunctional circuits have also been demonstrated based on graphene FETs, an amplifier with an actual voltage gain has not been realized because current saturation is difficult to obtain in graphene FETs owing to its zero band-gap.[18,24] Therefore, the CNT-based multifunctional FET actually is, in this capacity, superior to the graphene-based multifunctional FET.[16]

In fact, although low, the gain of the CNT amplifier can be further improved through certain strategies, including

optimizing the bias conditions, improving the transconductance through adopting a finger structure or building FETs based on CNTs arrays.[4,6,25] In addition, although our working frequency is on the kHz scale, the intrinsic frequency response of CNT can also be further improved. Owing to ultrahigh carrier mobility and saturation velocity, the potential work frequency of CNT FETs may reach up to THz regime.[5] Through some well-known methods to reduce the parasitic effects of CNT FETs, for example adopting CNTs arrays to reduce parasitic resistance,[4,6] high work frequency up to tens of GHz is expected in the CNT-based multifunctional ambipolar circuits.

The possibility of realizing multifunctionality on a single FET would provide tremendous flexibility and enhanced functionality for designing and building CNT FET-based RF circuits, for example, we can apply CNT FETs to realize frequency shift keying (FSK).[16] And if we cascade a device working in frequency doubler mode and a device working in amplifier mode, we are able to achieve actual amplification after frequency doubling, which is of more practical value than a single stage frequency doubler with small output signal amplitude.

3. Conclusions

Top-gated FETs have been fabricated on large diameter CNTs, which present typical ambipolar transfer characteristics. Depending on the DC biasing conditions, the ambipolar FETs can be used as the core to realize multifunctional AC circuits, including a high-efficiency ambipolar frequency doubler in the ambipolar transfer region, and an in-phase amplifier or inverted amplifier in the linear transfer regions. Taking advantages of the current saturation and large transconductance, an AC amplifier with a voltage gain of 2 was realized on the single CNT. The actual amplification (gain>1) and frequency doubling functions realized indicates that complicated radio frequency circuits or systems can be constructed based on this multifunctional transistor component.

4. Experimental Section

CNTs were grown via catalytic chemical vapor deposition (CVD) method on heavily doped silicon wafer, which was covered by a 500-nm-thick SiO_2 insulating layer.[26] All device patterns were defined via electron beam lithography (EBL, Raith Elphy Plus), and all the metal thin films were accomplished via e-beam evaporation (Kurt J. Lesker AXXIS). The source (S) and drain (D) electrodes consist of 30 nm Ti and 50 nm Au metal stack. The gate (G) stack consists of an atomic layer deposition (ALD, Cambridge Savannah) grown 12 nm HfO_2 and a 5/5 nm Ti/Au metal thin film. The diameter of the CNTs was measured from the line profile extracted from the atomic force microscope (AFM, Veeco Nanoman) height image. The electric measurements were carried out via a probe station in a vacuum chamber with 10^{-7} Torr base pressure (Lakeshore TTP-4). The DC measurements were based on Keithley 4200 semiconductor characterization system, and the AC measurement facilities include an Agilent 33220A signal generator, and an Agilent DSO7054A digital oscilloscope.

Acknowledgements

This work was supported by the Ministry of Science and Technology of China (Grant Nos. 2011CB933001 and 2011CB933002), and National Science Foundation of China (Grant No. 61071013).

Received: August 2, 2012
Published online: September 11, 2012

[1] P. Avouris, Z. H. Chen, V. Perebeinos, *Nat. Nanotechnol.* **2007**, *2*, 605.
[2] M. Burghard, H. Klauk, K. Kern, *Adv. Mater.* **2009**, *21*, 2586.
[3] F. Schwierz, *Nat. Nanotechnol.* **2010**, *5*, 487.
[4] C. Rutherglen, D. Jain, P. J. Burke, *Nat. Nanotechnol.* **2009**, *4*, 811.
[5] P. J. Burke, *Solid-State Electron.* **2004**, *48*, 1981.
[6] L. Nougaret, H. Happy, G. Dambrine, V. Derycke, J.-P. Bourgoin, A. A. Green, M. C. Hersam, *Appl. Phys. Lett.* **2009**, *94*, 243505.
[7] S. Rosenblatt, H. Lin, V. Sazonova, S. Tiwari, P. L. McEuen, *Appl. Phys. Lett.* **2005**, *87*, 153111.
[8] L. Liao, Y.-C. Lin, M. Q. Bao, R. Cheng, J. W. Bai, Y. Liu, Y. Q. Qu, K. L. Wang, Y. Huang, X. F. Duan, *Nature* **2010**, *467*, 305.
[9] Y. Q. Wu, K. A. Jenkins, A. Valdes-Garcia, D. B. Farmer, Y. Zhu, A. A. Bol, C. Dimitrakopoulos, W. J. Zhu, F. N. Xia, P. Avouris, Y.-M. Lin, *Nano Lett.* **2012**, *12*, 3062.
[10] Y.-M. Lin, A. Valdes-Garcia, S.-J. Han, D. B. Farmer, I. Meric, Y. N. Sun, Y. Q. Wu, C. Dimitrakopoulos, A. Grill, P. Avouris, K. A. Jenkins, *Science* **2011**, *332*, 1294.
[11] H. Wang, D. Nezich, J. Kong, T. Palacios, *IEEE Electron Device Lett.* **2009**, *30*, 547.
[12] Z. X. Wang, Z. Y. Zhang, H. L. Xu, L. Ding, S. Wang, L.-M. Peng, *Appl. Phys. Lett.* **2010**, *96*, 173104.
[13] H. Wang, A. Hsu, J. Wu, J. Kong, T. Palacios, *IEEE Electron Device Lett.* **2010**, *31*, 906.
[14] J. S. Moon, D. Curtis, D. Zehnder, S. Kim, D. K. Gaskill, G. G. Jernigan, R. L. Myers-Ward, C. R. Eddy Jr., P. M. Campbell, K.-M. Lee, P. Asbeck, *IEEE Electron Device Lett.* **2011**, *32*, 270.
[15] X. B. Yang, G. X. Liu, M. Rostami, A. A. Balandin, K. Mohanram, *IEEE Electron Device Lett.* **2011**, *32*, 1328.
[16] X. B. Yang, G. X. Liu, A. A. Balandin, K. Mohanram, *ACS Nano* **2010**, *4*, 5532.
[17] Z. X. Wang, L. Ding, T. Pei, Z. Y. Zhang, S. Wang, T. Yu, X. F. Ye, F. Peng, Y. Li, L.-M. Peng, *Nano Lett.* **2010**, *10*, 3648.
[18] S.-J. Han, K. A. Jenkins, A. Valdes-Garcia, A. D. Franklin, A. A. Bol, W. Haensch, *Nano Lett.* **2011**, *11*, 3690.
[19] T. Durkop, S. A. Getty, E. Cobas, M. S. Fuhrer, *Nano Lett.* **2004**, *4*, 35.
[20] J. H. Chen, C. Jang, S. D. Xiao, M. Ishigami, M. S. Fuhrer, *Nat. Nanotechnol.* **2008**, *3*, 206.
[21] Z. Y. Zhang, S. Wang, L. Ding, X. L. Liang, T. Pei, J. Shen, H. L. Xu, Q. Chen, R. L. Cui, Y. Li, L.-M. Peng, *Nano Lett.* **2008**, *8*, 3696.
[22] R. Saito, G. Dresselhaus, M. S. Dresselhaus, *Physical Properties of Carbon Nanotubes*, Imperial College Press, London **1998**.
[23] B. Razavi, *Design of Analog CMOS Integrated Circuits*, McGraw-Hill, New York **2001**.
[24] I. Meric, M. Y. Han, A. F. Young, B. Ozyilmaz, P. Kim, K. L. Shepard, *Nat. Nanotechnol.* **2008**, *3*, 654.
[25] L. Ding, Z. X. Wang, T. Pei, Z. Y. Zhang, S. Wang, H. L. Xu, F. Peng, Y. Li, L.-M. Peng, *ACS Nano* **2011**, *5*, 2512.
[26] Z. Jin, H. B. Chu, J. Y. Wang, J. X. Hong, W. C. Tan, Y. Li, *Nano Lett.* **2007**, *7*, 2073.